Investigation of Bakuchiol-Loaded Beads Synthesis Using Coaxial Electrospray and their Stability

Apisittipong Srinusud[1], *Tanawan* Boonmee[1], *Chayanee* Suwimon[1], and *Nisalak* Trongsiriwat[1*]
[1]Department of Industrial Chemistry, Faculty of Applied Science, King Mongkut's University of Technology North Bangkok, Wongsawang, Bangsue, 10800 Bangkok, Thailand

Abstract. Bakuchiol, a meroterpene derived from *Psoralea corylifolia*, offers diverse skin benefits but is prone to degradation under environmental stress. This study aimed to encapsulate bakuchiol in alginate-based beads using coaxial electrospray to enhance its stability. Bead formation was optimized by varying sodium alginate concentrations, core-to-shell flow rates, and applied voltage. Optimal conditions (1.0% w/v alginate; 20:40 mL/min; 1000 V) yielded spherical, well-defined beads. Fourier-transform infrared (FT-IR) spectroscopy confirmed successful encapsulation. Stability tests demonstrated that the beads maintained structural integrity and bakuchiol retention under various storage conditions over 60 days. High retention (greater than 80%) was achieved in neutral and moderately acidic pH (3, 5 and 7) solutions and under both light and dark storage, underscoring the protective role of the alginate matrix. Conversely, exposure to alkaline pH induced degradation and diffusion-related loss. These findings indicate that coaxial electrospray-based alginate beads represent a promising delivery system for stabilizing bakuchiol, supporting its future application in cosmetic formulations.

1 Introduction

Bakuchiol (BK) is a meroterpene extracted from the seeds of *Psoralea corylifolia* [1, 4-6]. It has garnered increasing attention in the cosmetics and cosmeceuticals industries due to its broad range of skin benefits. These include reducing hyperpigmentation, minimizing wrinkles [5, 7-9], enhancing skin elasticity [5], stimulating collagen production [9], antioxidant, anti-inflammatory [10, 11], anti-acne and anti-bacterial [10, 13, 14]. Importantly, bakuchiol exerts these bioactivities with low skin irritation relative to retinol, making it suitable for sensitive skin types [5, 15]. As a result, bakuchiol has emerged as a promising natural alternative to retinol in anti-aging formulations [8-10, 16].

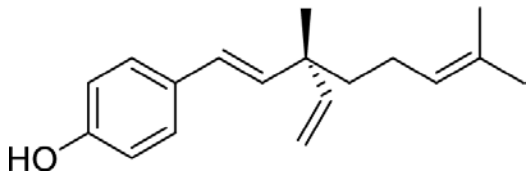

Fig. 1. Chemical structure of bakuchiol.

Chemically, bakuchiol (4-(3-ethenyl-3,7-dimethyl-1, 6-octadienyl)-phenol; $C_{18}H_{24}O$) [1] belongs to the meroterpenoid class, consisting of a phenolic group and an unsaturated hydrocarbon chain [1-4]. Due to its hydrophobic nature, bakuchiol dissolves readily in oils such as moringa and olive oil [16], as well as in organic solvents like ethanol and dimethyl sulfoxide (DMSO) [3, 11]. However, bakuchiol exhibits poor stability when exposed to light, oxygen, and heat, which can compromise its chemical integrity and biological efficacy [17-19].

Encapsulation technologies have been explored as a means of protecting active compounds from environmental degradation [20, 21]. Among various encapsulation approaches, polysaccharide-based systems are particularly attractive due to their biocompatibility and biodegradability [22]. Alginate, a natural polysaccharide derived from brown seaweed, is widely employed for encapsulation owing to its mild gelation process and excellent barrier properties [23, 24]. In the presence of calcium ions (Ca^{2+}), alginate chains undergo ionic crosslinking via interaction with guluronic acid residues, resulting in a dense and stable three-dimensional network commonly referred to as the "egg-box" structure [24, 25]. The alginate gel matrix offers mechanical stability and a protective barrier against external stressors [23, 26], making alginate an ideal candidate for encapsulating sensitive active ingredients like bakuchiol.

The coaxial electrospray technique offers an effective method for producing core–shell micro- and nanoparticles [27]. In this process, two immiscible liquids are co-delivered through a coaxial nozzle at controlled flow rates. When a high voltage is applied, the electric field overcomes the surface tension of the solution, generating a Taylor cone at the nozzle tip. This results in the emission of fine droplets toward the collector, typically containing a crosslinking solution [28]. The advantages of this

* Corresponding author : Nisalak.t@sci.kmutnb.ac.th

technique include high encapsulation efficiency, mild processing without heat, and the production of uniform particles [29-31].

This study provides a systematic investigation into the synthesis and stability of BK-loaded beads using coaxial electrospray. The primary objectives are to optimize the bead formation process, characterize the chemical and structural properties of the resulting beads, and evaluate the stability of encapsulated bakuchiol under various storage conditions including storage in calcium chloride solution and ultrapure water at room temperature under light and dark conditions, as well as in buffer solutions with pH values of 1, 3, 5, 7, and 9. Finally, the retained bakuchiol content in the beads was quantified. The insights gained from this work aim to support future applications in cosmetic formulations.

2 Materials and Methods

2.1 Materials

Bakuchiol was supplied from Chanjao Longevity Co. (Bangkok, Thailand). Sodium alginate, coconut oil and calcium chloride (food grade) were supplied from Krungthepchemi Co. (Bangkok, Thailand). Hydrochloric acid, sodium hydroxide, and methanol (AR grade) were supplied from Qrec Co. (New Zealand). Ultrapure water was obtained from the Department of Industrial Chemistry, Faculty of Applied Science, King Mongkut's University of Technology North Bangkok (KMUTNB).

2.2 Preparation of beads

Beads were prepared using a coaxial electrospray technique with a core-shell structure comprising an inner needle nested inside an outer needle. The core solution was prepared by dissolving bakuchiol in coconut oil at a concentration of 1% (v/v). The shell solution was prepared by dissolving sodium alginate in ultrapure water at concentrations of 1.0%, 1.5%, and 2.0% (w/w). A calcium chloride ($CaCl_2$) solution at 2.0% (w/v) was prepared in ultrapure water and used as the crosslinking bath to induce gelation during bead formation. The core and shell solutions were fed through a coaxial nozzle under controlled conditions. Details of the formulation and processing parameters are summarized in Table 1.

2.3 Fourier transform infrared spectroscopy

Fourier transform infrared (FT-IR) spectra were obtained using the PerkinElmer Spectrum 100 FT-IR Spectrometer to analyze the chemical composition of the prepared beads. The samples were prepared using the KBr pellet method. As the prepared beads were prone to moisture absorption, a drying process was required by placing them in a desiccator before grinding and compressing into transparent pellets. The pellets were scanned at a frequency of 4000-400 cm^{-1} for a total of 64 scans.

2.4 Optical microscope

The morphology of beads was characterized by optical microscope (Olympus). The beads were placed on a slide, then examined at 10X magnification.

Table 1. Process parameters for coaxial electrospray bead formation.

Parameters	Set	Unit
Bakuchiol; Core concentration	1	%w/v
Sodium alginate; Shell concentration	1, 1.5, 2	%w/v
$CaCl_2$; Collector concentration	1, 2, 3	%w/v
Flow rate of core	15, 20, 30	mL/min
Flow rate of shell	35, 40, 50	mL/min
Applied voltage	0, 1000	Volt
Frequency	400	Hz
Core diameter	450	µm
Shell diameter	700	µm

2.5 Determination of bakuchiol content in beads

The amount of bakuchiol encapsulated in the beads was determined using UV–Vis spectroscopy. The absorbance of the bead samples was measured at a wavelength of 262 nm on days 0, 14, 30, and 60. The bakuchiol content per bead (µg per bead) was quantified from a calibration curve prepared using standard bakuchiol solutions in methanol.

The percentage of bakuchiol retention was calculated according to the following equation:

$$\% \ Retention = (M_t / M_0) \times 100 \quad (1)$$

where M_t represents the bakuchiol content at each time point, and M_0 is the initial content at day 0.

2.6 Stability study

The stability of the beads during storage was evaluated under various conditions. The beads were immersed in calcium chloride solution, distilled water, and solutions with pH values of 1, 3, 5, 7, and 9. The samples were stored at room temperature. Sampling was conducted on days 0, 14, 30 and 60 to assess morphological changes and quantify the encapsulated compound.

2.7 Particle sizes of the beads

The particle sizes of the beads were characterized by capturing microscopic images and measuring the average bead diameter size using ImageJ software.

3 Results and Discussion

3.1 Formation of the beads

3.1.1 Effect of sodium alginate concentration and flow rates

The formation of beads was investigated by varying sodium alginate concentrations and core-to-shell flow rates. A bakuchiol concentration of 1.0% w/v was selected, along with a calcium chloride crosslinking bath at 2.0% w/v, an applied voltage of 1000 V, and a frequency of 400 Hz.

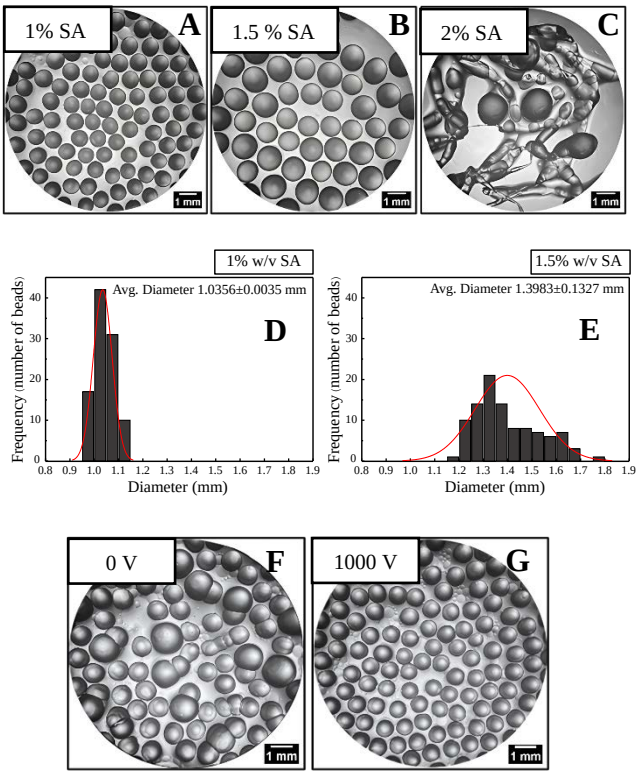

Fig. 2. Effect of sodium alginate concentration, flow rates, and applied voltage on bead formation. (A-C) Optical images of beads prepared with 1.0%, 1.5%, and 2.0% w/v sodium alginate; (D-E) size distribution of beads prepared with 1.0% and 1.5% w/v sodium alginate at optimal flow rates; (F-G) effect of applied voltage on bead morphology (F: 0 V, G: 1000 V).

The core-shell structures of the beads were clearly identified based on their morphological characteristics observed under optical microscopy. Optimal bead formation was observed at an alginate concentration of 1.0% w/v with a core-to-shell flow rate of 20:40 mL/min (Figure 2A), resulting in spherical beads with well-defined morphology and uniform size distribution. In contrast, lower flow rates (15:35 and 15:40 mL/min) produced beads with irregular shapes. At a higher flow rate of 30:50 mL/min, the shell layer appeared thick and uneven, and the core was inconsistently encapsulated, suggesting incomplete or unstable droplet formation. At an alginate concentration of 1.5% w/v (Figure 2B), the beads exhibited a broader size distribution, while at 2.0% w/v (Figure 2C), elongated and thread-like structures were observed, indicating that the higher solution viscosity hindered the formation of discrete droplets [25, 26].

3.1.2 Effect of applied voltage

The effect of applied voltage on the formation of alginate beads was investigated using sodium alginate concentrations of 1.0% w/v, with core-to-shell flow rate ratios of 20:40 mL/min. The crosslinking bath contained 2.0% w/v calcium chloride solution, and the electrospray frequency was fixed at 400 Hz.

At 0 V (Figure 2F), the electrospraying process failed to produce well-defined beads. Instead, irregular and aggregated structures were observed. This result is attributed to the absence of an electric field, which is critical for inducing the formation of a stable Taylor cone and promoting the breakup of the liquid into discrete droplets. In the absence of sufficient electrostatic repulsion, the droplets tended to coalesce upon contact, resulting in non-uniform bead morphology [32]. In contrast, applying a voltage of 1000 V (Figure 2G) yielded uniform, spherical beads. The applied electric field at this voltage promoted the formation of a stable Taylor cone at the nozzle tip, which led to the generation of a fine liquid jet that disintegrated into charged droplets. The mutual electrostatic repulsion between these charged droplets minimized aggregation and enabled uniform dispersion into the crosslinking bath. Additionally, the electric field accelerated the movement of the droplets toward the grounded collector, reducing the time available for droplet coalescence and allowing rapid gelation upon contact with the calcium chloride solution [33].

3.1.3 Effect of calcium chloride concentration

Beads were prepared using 1.0% w/v sodium alginate, a core-to-shell flow rate ratio of 20:40 mL/min, an applied voltage of 1000 V, and an electrospray frequency of 400 Hz. These parameters had previously produced well-defined core-shell structures.

Calcium chloride concentrations of 1.0%, 2.0%, and 3.0% w/v were tested. The mean bead diameter decreased from 1.081 mm at 1.0% calcium chloride to 0.945 mm at 3.0% (Figure 3). The decrease in bead size can be attributed to enhanced ionic crosslinking between calcium ions and the guluronic acid residues of sodium alginate, resulting in a dense gel network through the “egg-box” model. Stronger crosslinking produced smaller and more compact beads. These results confirm that calcium ion concentration is a key parameter for tuning particle morphology and size [34].

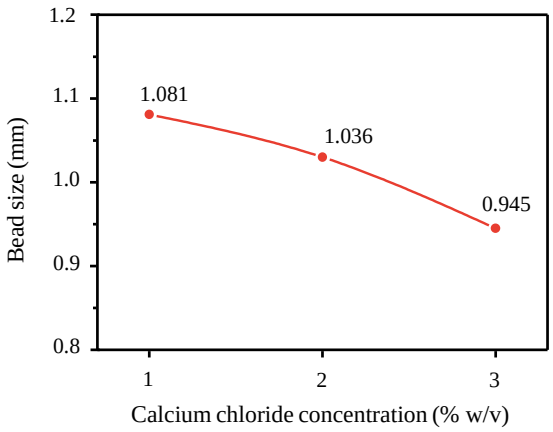

Fig. 3. Effect of calcium chloride concentration (1.0%, 2.0%, and 3.0% w/v) on the average bead diameter.

3.2 Fourier transform infrared spectroscopy

The FT-IR spectra of bakuchiol (a), sodium alginate (b), coconut oil (c), and the prepared beads (d) were displayed in Figure 4. The characteristic peaks of bakuchiol were observed at 3359.24 cm^{-1} (O–H stretching), 2966.08 cm^{-1} (C–H stretching), and 1632.48 cm^{-1} (C=C aromatic stretching). Sodium alginate showed characteristic peaks at 3445.95 cm^{-1} (O–H stretching), 2925.07 cm^{-1} (C–H stretching), 1614.89 cm^{-1} (asymmetric COO^- stretching), 1445.98 cm^{-1} (symmetric COO^- stretching), and 1031.78 cm^{-1} (C–O stretching). Coconut oil exhibited peaks at 3471.26 cm^{-1} (O–H stretching), 2854.04 cm^{-1} (C–H stretching), 1746.81 cm^{-1} (C=O stretching), 1465.80 cm^{-1} (C–H bending), and 1160.30 cm^{-1} (C–O stretching). When the prepared beads were characterized, the spectrum showed absorption bands at 3466.46 cm^{-1} (O–H stretching), 2854.26 cm^{-1} (C–H stretching), 1513.87 cm^{-1} (C–H bending), 1465.80 cm^{-1} (C–H bending), and 1160.45 cm^{-1} (C–O stretching), confirming the successful encapsulation of bakuchiol within the alginate beads.

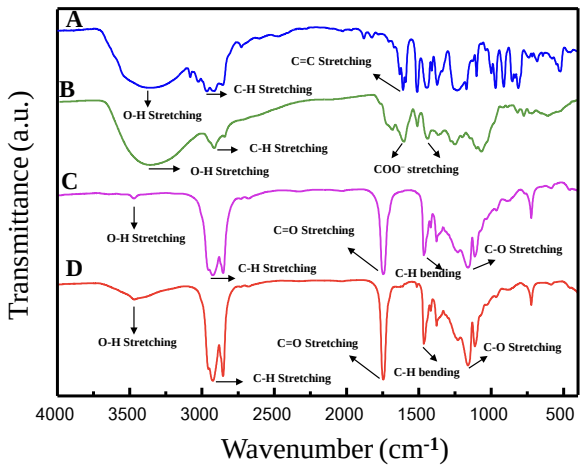

Fig. 4. FT-IR spectra of (A) bakuchiol, (B) sodium alginate, (C) coconut oil, and (D) prepared beads.

3.3 Stability under different conditions

3.3.1 Stability of beads in ultrapure water and calcium chloride solution

The stability of the prepared beads was evaluated over a 30-day storage period in both calcium chloride solution and ultrapure water (Figure 5). Beads stored in calcium chloride solution showed a gradual decrease in size over time. The bead diameter decreased from 1.024 mm at day 0 to 1.013 mm at day 30. This size reduction is attributed to the continued ionic crosslinking between calcium ions and the guluronic acid residues of sodium alginate in the shell layer. The formation of a more compact and ordered network, known as the "egg-box" structure, results in tighter packing of the polymer chains, thereby reducing the overall bead size. In contrast, swelling was observed in beads stored in ultrapure water, with bead size increasing from 1.027 mm at day 0 to 1.077 mm at day 30. The absence of calcium ions in the medium allows water to diffuse into the bead matrix, disrupting some of the ionic interactions and leading to minor expansion of the beads. The swelling is likely due to osmotic effects and water absorption within the alginate network [35, 36].

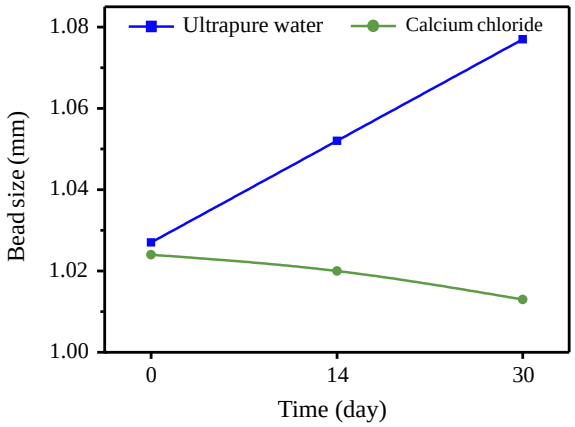

Fig. 5. Effect of storage solution (calcium chloride and ultrapure water) on the bead after 30 day storage.

3.3.2 Stability of beads in storage under light and dark conditions

The stability of BK-loaded beads was evaluated over a 60-day storage period under light and dark conditions at room temperature (Figure 6). The initial bakuchiol content was 6.53 µg per bead, corresponding to 100% remaining at day 0.

Under light exposure (Figure 6-A), the remaining bakuchiol content decreased to 99.68%, 95.65%, and 90.55% at days 14, 30, and 60, respectively. Similarly, under dark conditions (Figure 6-B), the remaining content was 99.85%, 95.66%, and 91.57% at days 14, 30, and 60. The similar degradation observed under both light and dark storage conditions suggests that light exposure had a minimal effect on the stability of bakuchiol within the alginate beads. The encapsulation provided sufficient protection against photo-degradation, likely due to the barrier properties of the alginate matrix. The gradual decrease in bakuchiol content over time can be attributed

to chemical degradation and possible diffusion-related loss, rather than light-induced effects. These findings indicate that the prepared beads effectively maintain bakuchiol stability under typical storage conditions.

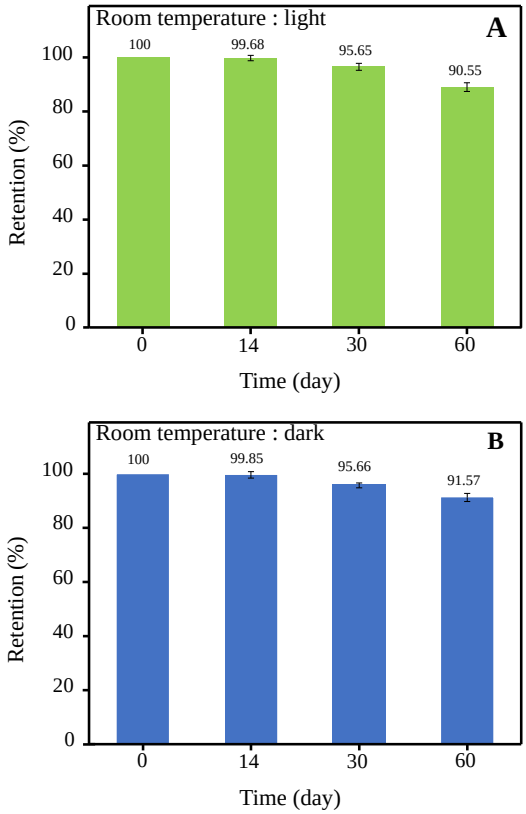

Fig. 6. Percentage of retention bakuchiol in beads during storage under (A) light and (B) dark conditions at room temperature after 60 day storage.

3.3.3 Stability of beads in different pH solutions

The stability of BK-loaded beads was evaluated in solutions of different pH values (pH 1, 3, 5, 7 and 9) over a 60-day storage period (Figure 7).

At neutral and acidic conditions (pH 3, pH 5, and pH 7), the beads maintained relatively high bakuchiol retention, with remaining content exceeding 80% after 60 days. In contrast, exposure to strongly basic conditions (pH 9) resulted in a more pronounced decrease in bakuchiol content, with values declining to below 60%. At alkaline pH, the alginate network may undergo swelling and partial decrosslinking due to ion exchange and matrix relaxation, which promotes the diffusion of the active compound out of the beads [37]. These findings suggest that the prepared beads effectively stabilize bakuchiol under neutral and moderately acidic conditions.

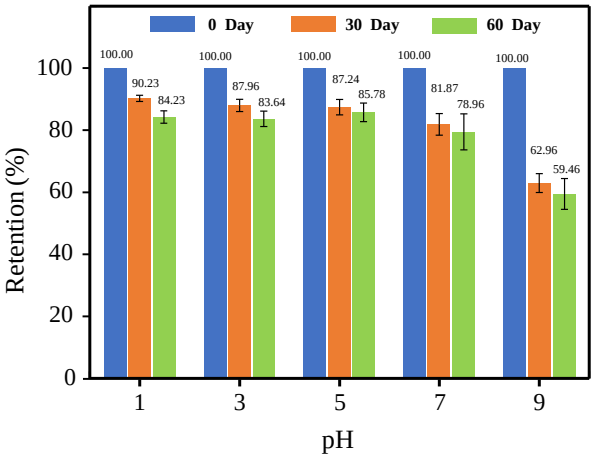

Fig. 7. Percentage of retention bakuchiol in beads after 0, 30, and 60 day storage in buffer solutions of different pH (pH 1, 3, 5, 7, and 9).

4 Conclusion

This study successfully demonstrated the synthesis of BK-loaded beads using coaxial electrospray, with systematic optimization of key processing parameters. Bead formation was highly dependent on sodium alginate concentration, core-to-shell flow rates, and applied voltage, with optimal conditions (1.0% w/v alginate; 20:40 mL/min flow rates; 1000 V) yielding spherical, well-defined beads with uniform size distribution. The Fourier transform infrared (FT-IR) spectroscopy confirmed the successful encapsulation of bakuchiol within the alginate gel matrix. Stability evaluations under various storage conditions revealed that the beads effectively maintained their structural integrity and bakuchiol content in both calcium chloride and ultrapure water over time. Furthermore, encapsulated bakuchiol exhibited high retention (greater than 80%) under neutral and moderately acidic conditions (pH 3, 5, and 7), and remained stable under both light and dark environments, highlighting the protective role of the alginate matrix. In contrast, exposure to alkaline pH led to increased degradation and potential diffusion-related loss. Overall, the findings indicate that coaxial electrospray-based alginate beads offer a promising delivery system for enhancing the stability of bakuchiol, supporting its future application in cosmetic formulations.

This research was supported by the Department of Industrial Chemistry, Faculty of Applied Science, King Mongkut's University of Technology North Bangkok. Special Thanks to Assoc. Prof. Dr. Sasithorn Kongruang for kindly providing the encapsulation machine to complete the research.

References

1. T. P. Adarsh Krishna, B. Edachery, S. Athalathil, Bakuchiol - a natural meroterpenoid, structure, isolation, synthesis and functionalization approaches. RSC Adv. **12**, 8815-8832 (2022). https://doi.org/10.1039/D1RA08771A
2. A. B. Lyons, I. Kohli, A. F. Nahhas, T. L. Braunberger, T. F. Mohammad, C. L. Nicholson, N. T. Nartker, K. Modi, M. S. Matsui, H.W. Lim, I. H. Hamzavi, Trichloroacetic acid model to accurately capture the efficacy of treatments for postinflammatory hyperpigmentation. Arch. Dermatol. Res. **312**, 437-446 (2020). https://doi.org/10.1007/s00403-020-02071-4
3. F. Mascarenhas-Melo, M.M. Ribeiro, K.H. Kahkesh, S. Parida, K.D. Pawar, K. Velsankar, A.C. Paiva-Santos, Comprehensive review of the skin use of bakuchiol, physicochemical properties, sources, bioactivities, nanotechnology delivery systems, regulatory and toxicological concerns. Phytochem. Rev. **23**, 1377-1413 (2024). https://doi.org/10.1007/s11101-024-09926-y
4. N. N. Nizam, S. Mahmud, S. M. A. Ark, M. Kamruzzaman, M. K. Hasan, Bakuchiol, a natural constituent and its pharmacological benefits. F1000Res. **12**, 29 (2023). https://doi.org/10.12688/f1000research.129072.2
5. R. K. Chaudhuri, K. Bojanowski, Bakuchiol, a retinol-like functional compound revealed by gene expression profiling and clinically proven to have anti-aging effects. Int. J. Cosmet. Sci. **36**, 221-230 (2014). https://doi.org/10.1111/ics.12117
6. J. Greenzaid, A. Friedman, P. Sodha, The use of bakuchiol in dermatology, a review of in vitro and in vivo evidence. J. Drugs Dermatol. 21, 624-629 (2022). https://doi.org/10.36849/JDD.6740
7. C. Puyana, N. Chandan, M. Tsoukas, Applications of bakuchiol in dermatology, systematic review of the literature. J. Cosmet. Dermatol. **21**, 6636-6643 (2022). https://doi.org/10.1111/jocd.15420
8. S. Dhaliwal, I. Rybak, S. R. Ellis, M Notay, M Trivedi, W Burney, A R Vaughn, M Nguyen, P Reiter, S Bosanac, H Yan, N Foolad, R K Sivamani, Prospective, randomized, double-blind assessment of topical bakuchiol and retinol for facial photoageing. Br. J. Dermatol. **180**, 289-296 (2019). https://doi.org/10.1111/bjd.16918
9. M. Kuśmierska, J. Kuśmierski, A. Martyka, P. Ujma, Redefining skin health, the potential of plant-based bakuchiol as a sustainable substitute for retinoids. Our Dermatol. Online **15**, 345-348 (2024). https://doi.org/10.7241/ourd.20244.3
10. A. Bluemke, A. P. Ring, J. Immeyer, A. Hoff, T. Eisenberg, W. Gerwat, F. Meyer, S. Breitkreutz, L.M. Klinger, J.M. Brandner, G. Sandig, M. Seifert, D. Segger, F. Rippke, Multidirectional activity of bakuchiol against cellular mechanisms of facial ageing - Experimental evidence for a holistic treatment approach. Int. J. Cosmet. Sci. **44**, 377-393 (2022). https://doi.org/10.1111/ics.12784
11. S. Adhikari, R. Joshi, B. S. Patro, T. K. Ghanty, G. J. Chintalwar, A. Sharma, S. Chattopadhyay, T. Mukherjee, Antioxidant activity of bakuchiol, experimental evidences and theoretical treatments on the possible involvement of the terpenoid chain. Chem. Res. Toxicol. **16**, 1062-1069 (2003). https://doi.org/10.1021/tx034082r
12. S. Y. Choi, S. Lee, W.-H. Choi, Y. Lee, Y.O. Jo, T.-Y. Ha, Isolation and anti-inflammatory activity of Bakuchiol from Ulmus davidiana var. japonica. J. Med. Food. **13**, 1019-1023 (2010). https://doi.org/10.1089/jmf.2009.1207
13. Y. Cui, X. Zeng, Y. Zeng, Q. Liu, H. Zeng, Constituents of Psoralea corylifolia Fruits and Their Effects on Methicillin-Resistant Staphylococcus aureus. Molecules. **20**, 12500-12511 (2015). https://doi.org/10.3390/molecules200712500
14. R. Chaudhuri, F. Marchio, Bakuchiol in the management of acne-affected skin. Cosmet. Toilet. **126**, 502-510 (2011).
15. Z.D. Draelos, H. Gunt, J. Zeichner, S. Levy, Clinical Evaluation of a Nature-Based Bakuchiol Anti-Aging Moisturizer for Sensitive Skin. J. Drugs Dermatol. **19**, 1181-1183 (2020). https://doi.org/10.36849/JDD.2020.5522
16. M. Hadiwidjaja, E. Romadhona, Y. Yulianto, N.A. Chauwito, M.G.E. Sidauruk, R. Kardiono, C. Avanti, Comparative efficacy of bakuchiol oil and encapsulated bakuchiol cream on facial skin quality: A 28-day pilot study. J. Pharm. Pharmacogn. Res. **12**, 477-486 (2024). https://doi.org/10.56499/jppres23.1812_12.3.477
17. N. Inmuangkham, P. Sukjarernchaikul, S. Thepwatee, Fatty acid profiles of olive oil and moringa oil and their influence on nanoemulsion formation via D-phase emulsification using bakuchiol as a model active compound. Ind. Crops Prod. **209**, 118052 (2024). https://doi.org/10.1016/j.indcrop.2024.118052
18. G. Wadhwa, S. Kumar, V. Mittal, R. Rao, Encapsulation of babchi essential oil into microsponges: Physicochemical properties, cytotoxic evaluation and anti-microbial activity. J. Food Drug Anal. **27**, 60-70 (2019). https://doi.org/10.1016/j.jfda.2018.07.006
19. K. Kurpet, G. Chwatko, Development of a new chromatographic method for the determination of bakuchiol in cosmetic products. Sci. Rep. **13**, 13893 (2023). https://doi.org/10.1038/s41598-023-41076-7
20. A. Rezagholizade-Shirvan, M. Soltani, S. Shokri, R. Radfar, M. Arab, E. Shamloo, Bioactive compound encapsulation: Characteristics, applications in food systems, and implications for human health. Food Chem.: X**.** **24**, 101953 (2024). https://doi.org/10.1016/j.fochx.2024.101953
21. M. Figueiredo, Z. Sárkány, F. Rocha, P. M. Martins, Challenges and Advances in the Encapsulation of Bioactive Ingredients Using Whey Proteins. Foods. **14**, 691 (2025). https://doi.org/10.3390/foods14040691

22. P. M. Junaid, S. Ali, K. Rasul, A. Abdullah, Polysaccharide-based hydrogels for microencapsulation of bioactive compounds: A review. J. Agric. Food Res. **15**, 101038 (2024). https://doi.org/10.1016/j.jafr.2024.101038
23. K. Y. Lee, D. J. Mooney, Alginate: properties and biomedical applications. Prog. Polym. Sci. **37**, 106-126 (2012). https://doi.org/10.1016/j.progpolymsci.2011.06.003
24. K. I. Draget, G. Skjåk-Braek, O. Smidsrød, Alginate based new materials. Int. J. Biol. Macromol. **21**, 47-55 (1997). https://doi.org/10.1016/s0141-8130(97)00040-8
25. G. T. Grant, E. R. Morris, D. A. Rees, P. J. C. Smith, D. Thom, Biological interactions between polysaccharides and divalent cations: The egg-box model. FEBS Lett. **32**, 195-198 (1973). https://doi.org/10.1016/0014-5793(73)80770-7
26. D. Zadeike, Z. Gaizauskaite, L. Basinskiene, R. Zvirdauskiene, D. Cizeikiene, Exploring Calcium Alginate-Based Gels for Encapsulation of Lacticaseibacillus paracasei to Enhance Stability in Functional Breadmaking. Gels. **10**, 641 (2024). https://doi.org/10.3390/gels10100641
27. A. Arevalo-Gallegos, S. P. Cuellar-Bermudez, E. M. Melchor-Martinez, H. M. N. Iqbal, R. Parra-Saldivar, Comparison of Alginate Mixtures as Wall Materials of Schizochytrium Oil Microcapsules Formed by Coaxial Electrospray. Polymers. **15**, 2756 (2023). https://doi.org/10.3390/polym15122756
28. A. Letocha, M. Miastkowska, E. Sikora, Preparation and Characteristics of Alginate Microparticles for Food, Pharmaceutical and Cosmetic Applications. Polymers. **14**, 3834 (2022). https://doi.org/10.3390/polym14183834
29. L. G. Gómez-Mascaraque, F. Tordera, M. J. Fabra, M. Martínez-Sanz, A. Lopez-Rubio, Coaxial electrospraying of biopolymers as a strategy to improve protection of bioactive food ingredients. Innov. Food Sci. Emerg. Technol. **51,** 2-11 (2019). https://doi.org/10.1016/j.ifset.2018.03.023
30. C. Chen, W. Liu, P. Jiang, T. Hong, Coaxial Electrohydrodynamic Atomization for the Production of Drug-Loaded Micro/Nanoparticles. Micromachines**. 10**, 125 (2019). https://doi.org/10.3390/mi10020125
31. S. Tsai, Y. Ting, Synthesize of alginate/chitosan bilayer nanocarrier by CCD-RSM guided co-axial electrospray: A novel and versatile approach. Food Res. Int. **116**, 1163-1172 (2019). https://doi.org/10.1016/j.foodres.2018.11.047
32. A. M. Gañán-Calvo, J. M. Montanero, Revision of Capillary Cone-Jet Physics: Electrospray and Flow Focusing. Phys. Rev. E. **79**, 066305 (2009). https://doi.org/10.1103/PhysRevE.79.066305
33. M. R. Shaiqah, H. M. Salahuddin, A. Y. A. Huda, M. Izzuddin, N. I. M. N. Shafiq, M. A. N. Hakimah, S. R. Rahman, A. A. Budipratama, Screening of Electrospray-operating Parameters in the Production of Alginate-Royal Jelly Microbeads Using Factorial Design. J. Pharm. Bioallied Sci. **12**, S703-S706 (2020). https://doi.org/10.4103/jpbs.JPBS_249_19
34. C. Bennacef, A. Karim, S. El-Khaldi, M. Benyoussef, Influence of Alginate Properties and Calcium Chloride Concentration on Alginate Bead Reticulation and Size: A Phenomenological Approach. Polymers. **15**, 4163 (2023). https://doi.org/10.3390/polym15204163
35. S. K. Bajpai, R. Tankhiwale, Investigation of water uptake behavior and stability of calcium alginate/chitosan bi-polymeric beads: Part-1. React. Funct. Polym. **66**, 645-658 (2006). https://doi.org/10.1016/j.reactfunctpolym.2005.10.017
36. S.-L. Huang, Y.-S. Lin, The Size Stability of Alginate Beads by Different Ionic Crosslinkers. Adv. Mater. Sci. Eng. **2017**, 1-7 (2017). https://doi.org/10.1155/2017/9304592
37. N. Stachowiak, A. Kowalska, P. Zieliński, E. Romanowska, Stability Studies, Biodegradation Tests, and Mechanical Properties of Sodium Alginate and Gellan Gum Beads Containing Surfactant. Polymers. **15**, 2568 (2023). https://doi.org/10.3390/polym15112568